Intra/Inter Chip Wireless Interconnect System for ULSI (4)
－Low-k/Cu Interconnect－

Takamaro Kikkawa (Professor, Research Center for Nanodevices and Systems,
Graduate School of Advanced Sciences of Matter),
Susumu Sakamoto (Graduate School of Advanced Sciences of Matter, M2)

1. Research Target

According to the scaling rule [1] for miniaturization of the ultra-large-scale-integrated circuits (ULSI), the interconnect feature sizes of lines and spaces should be reduced. However, the increase of interconnect RC-delay, resistance-capacitance product occurs, therefore, the interconnect technology with low-resistance metal wire and low-dielectric constant (low-k) interlayer film are needed for ULSI. The purpose of this research is to develop low-k interlayer dielectric films with photosensitivity so that low-cost multilevel interconnect systems can be realized.

2. Research Results

Methylsilsesquioxane (MSQ) has been developed as a low dielectric constant material; k=2.7 [2,3]. Methylsilsesquiazane (MSZ) is a precursor component of MSQ as shown in Fig. 1. When the photo-acid generator (PAG) molecule is added to MSZ, it acquires the photosensitivity. The photosensitive MSZ precursor has sensitivity to not only ultra-violet light and but also electron-beam. Then the lithography of photosensitive low-k MSQ was examined by using ultra-violet light, KrF excimer laser, electron beam and SOR X-ray [3-5]. In these lithographies via and trench patterns were formed directly in the MSZ film without using dryetching. The dryetch-less process eliminates the resist coating and ashing, so that it can reduce process steps. Furthermore, the reliability issues such as void formation in the film due to dryetching and ashing [6] can be eliminated. At the same time disuse of hardmask and etch-stop layer enables us to reduce effective dielectric constant of multilevel interconnect interlayer.

MSZ is the precursor component of MSQ as shown in Fig. 1. When the photoacid generator (PAG) molecule is added to MSZ, and MSZ acquires photosensitivity. We call this chemical mixture photosensitive MSZ (PS-MSZ). The PAG molecule releases proton upon ultraviolet ray exposure or electron-beam exposure. The activated proton from the PAG attacks the bonds of its neighboring molecules and chemical reactions are provoked. Then in the exposed region of PS-MSZ film the protons attack Si-NH bonds, and frequently cut this bond. If water, H_2O, is present, Si-NH bond is replaced with Si-OH bond as shown in Fig 2. These microscopic reactions are repeated, and MSZ polymers in the exposed region are cut into small pieces. Along the exposed region of the film, macroscopic patterns are formed.

Reaction path of photosensitive MSZ is shown in Fig. 3. k_1, k_{-1} and k_2 are the rate constants, and which determine the reaction rate of patterning. From these equations, probability function of film patterning is calculated as

$$P(t) = 1 - \exp(-\gamma t), \qquad (1)$$

where

$$\gamma = \left(1 - \frac{k_{-1}}{k_{-1} + k_2[H_2O]}\right) \cdot k_1[H^+]. \qquad (2)$$

The concentrations are governed by the diffusion equation, and then the probability function is dependent on diffusion time and film location. The SEM micrographs of in a conventional process are shown in Fig. 4. Calculated pattern was fitted to these SEM micrographs, and the calculated patterns are given as Fig. 5. Since the energy of the electron beam is 50 keV, protons are distributed around the exposed pattern from the film surface to the bottom, and in subsequent humidification treatment the water diffuses into the MSZ film from the film surface. The H_2O concentration becomes lower level from the film surface to the bottom, and then threshold H_2O concentration determines the development of exposure pattern. An improved process performed uniform H_2O concentration. The calculation of the patterning probability predicts that an improved process can form abrupt pattern shapes. The SEM micrographs of photosensitive MSZ precursor in the improved process are shown in Fig. 6. It is found that the improved process formed abrupt pattern shapes. The minimal developed feature size was 90 nm at 111 μ C/cm^2. This feature size gives the aspect ratio 3.9.

The characteristics of photosensitive porous low-k methylsilsesquioxane (MSQ) were investigated by electron-beam lithography. Pore size distributions were measured by X-ray scattering measurement (XRS) using a Rigaku ATX-E X-ray diffractometer, as shown in Fig. 7. Peak pore radii for photosensitive porous MSQ with 10 wt% porogen and with 20 wt% porogen were 1.37 nm and 2.03 nm, respectively. Average pore radii for photosensitive porous MSQ with 10 wt% porogen and with 20 wt% porogen were 2.30 nm and 3.72 nm, respectively. The dielectric constant of photosensitive MSQ decreased with increasing porogen concentration, as shown in Fig. 8. The dielectric constants for photosensitive MSQ without porogen, with 10 wt% porogen and with 20 wt% porogen, measured by capacitance-voltage (CV) measurement, were 3.25, 3.05 and 2.73, respectively. The effective medium approximation (EMA) method predicts the reduction of dielectric constant with increasing porosity. The dielectric constant of EMA is given by the equation [7],

$$k_p = \frac{(k_s + 2) + 2(1 - x)(k_s - 1)}{(k_s + 2) - (1 - x)(k_s - 1)}, \qquad (3)$$

where k_p and k_s are the dielectric constants of the porous film and its skeleton, respectively, and x is porosity. EMA-calculated dielectric constants are shown in Fig. 8. In the EMA calculation, porosity values were given by the measured values of spectroscopic ellipsometry. It is found that the results of CV measurement were consistent with the EMA-calculated values. The difference between the measured value and EMA-calculated value could be attributed to the absorption of moisture in the porous films [8]. SEM images of photosensitive MSZ with and without porogen, and cured photosensitive porous MSQ are shown in Fig. 9. In micrographs of photosensitive porous MSZ (Fig. 9(b)), it is found that the porogen residue remained on the sidewall of the trench patterns. This is because porogen additives do not dissolve in the TMAH developer. Porogen evaporated at the 400℃ curing process, and then the porogen residue disappeared after 400℃ curing, as shown in Fig. 9(c). Then line-and-space patterns in the photosensitive porous MSQ film were formed by electron-beam lithography without dry etching.

3. **Summary and Future Plan**

Characteristics of photosensitive MSQ low-k film were investigated using electron-beam lithography. The process parameters to define the exposure pattern were investigated. In the post-humidification process the critical dimensions of the exposed patterns were dependent on the hold time from electron-beam exposure to humidification treatment. Diffusion of H_2O molecules from the film surface limited the development of the exposure patterns, resulting in tapered shape patterns. On the contrary, in the improved process the developed pattern showed abrupt shape. This is because H_2O concentration was uniform in photosensitive MSZ film. Consequently, abrupt shape of the pattern with high aspect ratio was achieved. In this process the aspect ratio was 3.9, and the minimal feature size was 90 nm.

A novel photosensitive porous MSQ interlayer dielectric film was developed. Photosensitive porous MSQ (20 wt% porogen) had a porosity of 17%, a pore radius of 2.2 nm, and a dielectric constant of 2.62. The characteristics of the photosensitive porous MSQ film were investigated, and the 50-200 nm photosensitive porous MSQ patterns could be formed successfully by electron-beam lithography without dry etching.

4. References

[1]. R.H. Dennard, F.H. Gaensslen, H-N. Yu, V.L. Rideout, E. Bassous and A.R. LeBlanc: IEEE J. Solid-State Circuits 9 (1974) 6.
[2]. S. Mukaigawa, T. Aoki, Y. Shimizu and T. Kikkawa: Jpn. J. Appl. Phys. 39(2000) 2189.
[3]. T. Kikkawa, T. Nagahara and H. Matsuo: Appl. Phys. Lett. 78 (2001)2557.
[4]. M. Tada, T. Ogura, and Y. Hayashi: Extended Abstracts of the 2002 Int. Conf. Solid State Devices and Materials, (2002) 44.
[5]. S. Kuroki, T. Kikkawa, H. Kochiya and S. Shishiguchi: Jpn. J. Appl. Phys. 42(2003) 1907.
[6]. A. Matsushita, N. Ohashi, K. Inukai, H. J. Shin, S. Sone, K. Sudou, K. Misawa, I. Matsumoto and N. Kobayashi: Proc. IITC (2003) 147.
[7]. N. Hata, C. Negoro, K. Yamada, H. S. Zhou, Y. Oku and T. Kikkawa: Extended Abstracts of the 2002 Int. Conf. Solid State Devices and Materials, (2002) 496.
[8]. S. Sakamoto, S. Kuroki and T. Kikkawa: Extended Abstracts of the 2003 Int. Conf. Solid State Devices and Materials, (2003) 478-479.

5. Achievement

Published papers

1. S. Kuroki, T. Kikkawa, H. Kochiya and S. Shishiguchi, "Low-k Dielectric Film Patterning by X-Ray Lithography", Jpn. J. Appl. Phys. Vol. 42 (2003), pp. 1907-1910.

2. S. Kuroki, S. Sakamoto and T. Kikkawa, "A Novel Photosensitive Porous Low-k Interlayer Dielectric Film", Jpn. J. Appl. Phys. Vol. 42 (2004), pp 1820-1824.

Proceedings

3. S. Kuroki, T. Kikkawa, H. Kochiya and S. Shishiguchi, "Direct Patterning of Low-k Dielectric Films using X-ray Lithography", Extended Abstracts of the 2004 International Conference on Solid State Devices and Materials, pp.464-465

4. S. Kuroki, T. Hirota and T. Kikkawa, "A Novel Photosensitive Porous Low-k Interlayer Dielectric Film", Extended Abstracts of the 2003 International Conference on Solid State Devices and Materials, pp.468-469.

5. S. Sakamoto, S. Kuroki and T. Kikkawa, “Influence of Humidity on Electrical Characteristics of Porous Silica Films”, Extended Abstracts of the 2003 Int. Conf. Solid State Devices and Materials, (2003) 478-479.

6. S. Kuroki, S. Sakamoto and T. Kikkawa, "Direct Patterning of Photosensitive Porous Low-k Film and Its Electrical Characteristics", Proceedings of The 65th Symposium on Semiconductors and Integrated Circuits Technology, pp.468-469.

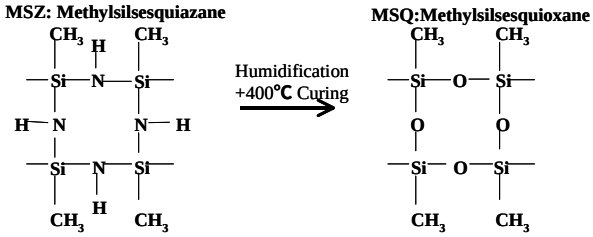

Fig.1. The chemical structure of MSZ-MSQ

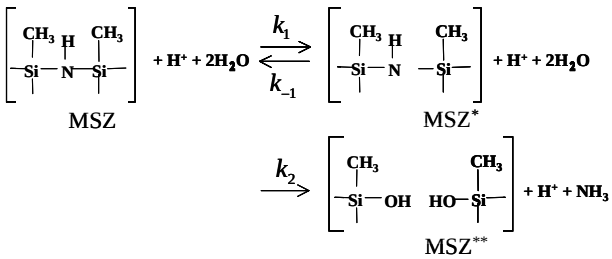

Fig. 3. Reaction path for photosensitive MSZ: MSZ^* shows mol concentration of the activated Si-N-Si bond. MSZ^{**} is mol concentration of broken Si-N-Si bond. , and are the reaction rates for each reaction.

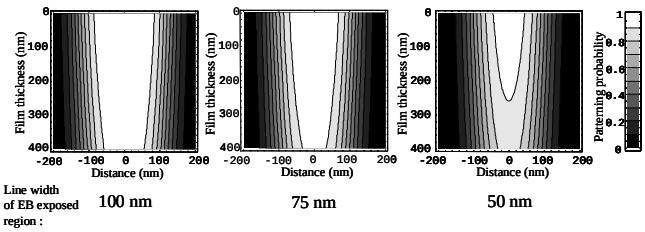

Fig. 5. Reaction probability as a function of EB exposed line width in the post-humidification process: it is found that the exposed pattern form is dependent on the line width. (H^+ diffusion time: 1420 sec, H_2O diffusion time: 180 sec)

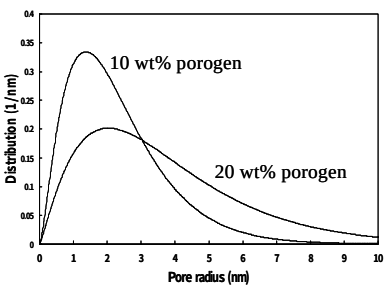

Fig.7. Pore radius distribution of photosensitive porous MSQ: peak pore radii of photosensitive porous MSQ with 10 wt% porogen and 20 wt% porogen were 1.37 nm and 2.03 nm, respectively.

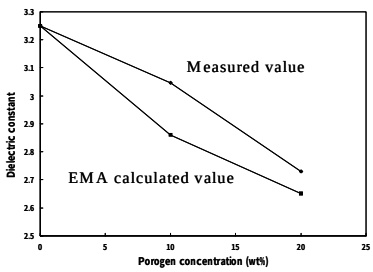

Fig.8. Dielectric constants of photosensitive porous MSQ: the dielectric constant of photosensitive MSQ decreased with increasing porogen concentration.

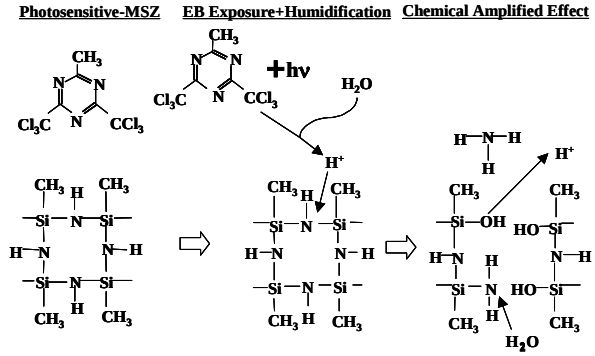

Fig. 2. Schematic diagram of photo-amplified reaction in photosensitive MSZ film.

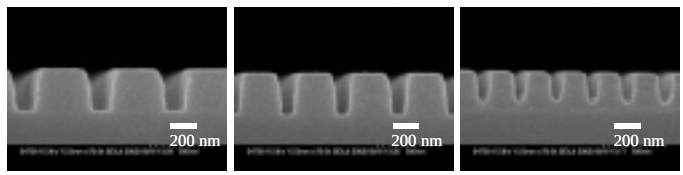

(a) 100 nm (b) 75 nm (c) 50 nm

Fig. 4. SEM micrographs of photosensitive MSZ in an conventional process. The lengths given below the images are the design sizes.

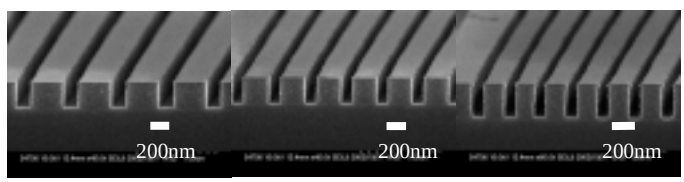

(a) 100 nm (b) 75 nm (c) 50 nm

Fig. 6. SEM micrographs of photosensitive MSZ in an improved process (exposure dose: 111 μC/cm2, L/S=1:5) . The lengths given below the images are the design sizes.

(a) Photosensitive MSZ without porogen

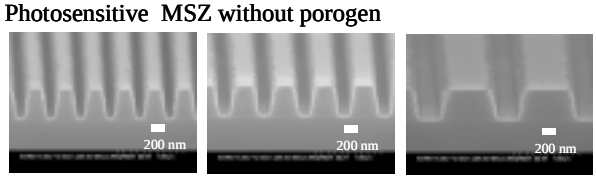

Design Size: 75 nm 100 nm 200 nm

(b) Photosensitive MSZ with porogen (10 wt% porogen)

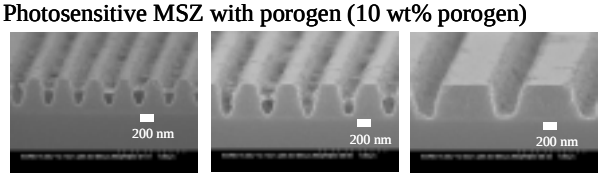

Design Size: 75 nm 100 nm 200 nm

(c) 400 ℃ Cured photosensitive porous MSQ (10 wt% porogen)

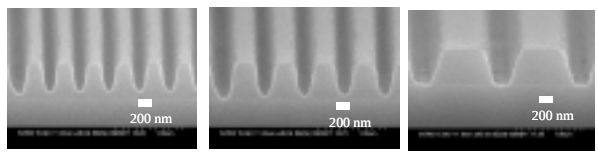

Design Size: 75 nm 100 nm 200 nm

Fig. 9. SEM micrographs of photosensitive porous MSQ: (a) photosensitive MSZ without porogen, (b) photosensitive MSZ with 10 wt % porogen and (c) cured photosensitive porous MSQ (10 wt% porogen). The electron beam exposure dose was 9.0 μC/cm^2.